



Solar-Powered Light Emitting Diode Power Line Avoidance Marker Design

By

**Ellen H. Snook
Clarence E. Rash
John S. Martin
Richard R. Levine**

Sensory Research Division

**Parley P. Johnson
James A. Lewis
John H. Hapgood**

Research Systems Division

December 1992

Approved for public release; distribution unlimited.

**U.S. Army Aeromedical Research Laboratory
Fort Rucker, Alabama 36362-0577**

Notice

Qualified requesters

Qualified requesters may obtain copies from the Defense Technical Information Center (DTIC), Cameron Station, Alexandria, Virginia 22314. Orders will be expedited if placed through the librarian or other person designated to request documents from DTIC.

Change of address

Organizations receiving reports from the U.S. Army Aeromedical Research Laboratory on automatic mailing lists should confirm correct address when corresponding about laboratory reports.

Disposition

Destroy this report when it is no longer needed. Do not return to the originator.

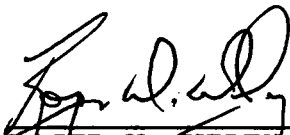
Disclaimer

The views, opinions, and/or findings contained in this report are those of the author(s) and should not be construed as an official Department of the Army position, policy, or decision, unless so designated by other official documentation. Citation of trade names in this report does not constitute an official Department of the Army endorsement or approval of the use of such commercial items.

Reviewed:



RICHARD R. LEVINE
LTC, MS
Director, Sensory Research
Division



ROGER W. WILEY, O.D., Ph.D.
Chairman, Scientific
Review Committee

Released for publication:



DAVID H. KARNEY
Colonel, MC, SFS
Commanding

REPORT DOCUMENTATION PAGE

Form Approved
OMB No. 0704-0188

| | | | | | |
|---|-------|---|--|--|-----------------------------------|
| 1a. REPORT SECURITY CLASSIFICATION Unclassified | | | 1b. RESTRICTIVE MARKINGS | | |
| 2a. SECURITY CLASSIFICATION AUTHORITY | | | 3. DISTRIBUTION / AVAILABILITY OF REPORT Approved for public release; distribution unlimited | | |
| 2b. DECLASSIFICATION / DOWNGRADING SCHEDULE | | | | | |
| 4. PERFORMING ORGANIZATION REPORT NUMBER(S) USAARL Report No. 93-6 | | | 5. MONITORING ORGANIZATION REPORT NUMBER(S) | | |
| 6a. NAME OF PERFORMING ORGANIZATION U.S. Army Aeromedical Research Laboratory | | 6b. OFFICE SYMBOL (If applicable) SGRD-UAS-VS | 7a. NAME OF MONITORING ORGANIZATION U.S. Army Medical Research and Development Command | | |
| 6c. ADDRESS (City, State, and ZIP Code) P.O. Box 577 Fort Rucker, AL 36362-5292 | | | 7b. ADDRESS (City, State, and ZIP Code) Fort Detrick Frederick, MD 21702-5012 | | |
| 8a. NAME OF FUNDING / SPONSORING ORGANIZATION | | 8b. OFFICE SYMBOL (If applicable) | 9. PROCUREMENT INSTRUMENT IDENTIFICATION NUMBER | | |
| 8c. ADDRESS (City, State, and ZIP Code) | | | 10. SOURCE OF FUNDING NUMBERS | | |
| | | | PROGRAM ELEMENT NO. 0602787A | PROJECT NO. 3M162 787879 | TASK NO. BG |
| | | | | | WORK UNIT ACCESSION NO. 164 |
| 11. TITLE (Include Security Classification) (U) Solar-Powered Light Emitting Diode Power Line Avoidance Marker Design | | | | | |
| 12. PERSONAL AUTHOR(S) Snook, Ellen H.; Rash, Clarence E.; Martin, John S.; Levine, Richard R.; Johnson, Parley P.; Lewis, James A.; Hapgood, John H. | | | | | |
| 13a. TYPE OF REPORT Final | | 13b. TIME COVERED FROM _____ TO _____ | | 14. DATE OF REPORT (Year, Month, Day) 1992 December | |
| | | | | 15. PAGE COUNT 25 | |
| 16. SUPPLEMENTARY NOTATION | | | | | |
| 17. COSATI CODES | | | 18. SUBJECT TERMS (Continue on reverse if necessary and identify by block number) | | |
| FIELD | GROUP | SUB-GROUP | wire marker, light emitting diode, solar power, aided and unaided flights | | |
| 20 | 06 | | | | |
| 23 | 02 | | | | |
| 19. ABSTRACT (Continue on reverse if necessary and identify by block number) In-flight wire strikes are a constant threat to U.S. Army Aviation during all-weather, daytime and nighttime helicopter operations. Despite routine training on wire avoidance techniques, wire strikes continue to occur, with a majority of the mishaps historically occurring during training and maneuvering over familiar sites. In an effort to increase the conspicuity of suspended cables and wires, the aviation training community at Fort Rucker, Alabama, currently employs a passive wire marking system which consists of international-orange colored spheres suspended from cables and wires in heavily trafficked airspace. During a previous evaluation of wire marker visibility, a solar-powered wire marker design was developed. This new design incorporates retroreflective material and light emitting diodes (LEDs) to provide greater range visibility and detectability during aided and unaided flight. | | | | | |
| 20. DISTRIBUTION / AVAILABILITY OF ABSTRACT <input checked="" type="checkbox"/> UNCLASSIFIED/UNLIMITED <input type="checkbox"/> SAME AS RPT. <input type="checkbox"/> DTIC USERS | | | 21. ABSTRACT SECURITY CLASSIFICATION Unclassified | | |
| 22a. NAME OF RESPONSIBLE INDIVIDUAL Chief, Scientific Information Center | | | 22b. TELEPHONE (Include Area Code) 205-255-6907 | | 22c. OFFICE SYMBOL SGRD-UAX-SI |

Table of contents

Page

| | |
|---|-----|
| List of figures..... | ii |
| List of tables..... | ii |
| Acknowledgments..... | iii |
| Introduction..... | 1 |
| Technical description..... | 5 |
| System description and operation..... | 5 |
| Circuit description and operation..... | 7 |
| Bench test..... | 10 |
| Field test..... | 11 |
| Detection performance..... | 11 |
| Operational performance..... | 14 |
| Summary..... | 17 |
| Reference..... | 19 |
| Appendix A - List of manufacturers..... | 20 |
| Appendix B - List of components..... | 21 |

List of figures

| Figure no. | | Page |
|------------|---|------|
| 1 | Current basic wire marker (international-orange sphere) mounted on power line..... | 2 |
| 2 | Wire marker test designs: (a) current uniform sphere, (b) modified sphere with reflective tape in a cross (X) pattern, (c) uniform polyhedron, (d) polyhedron with circular retroreflective tape..... | 2 |
| 3 | Exterior view of solar-powered light emitting diode wire marker design..... | 6 |
| 4 | Interior view of solar-powered light emitting diode wire marker design..... | 6 |
| 5 | Wire marker design functional block diagram..... | 7 |
| 6 | Schematic of solar-powered light emitting diode wire marker design..... | 8 |
| 7 | Output voltage plots for bench test..... | 12 |
| 8 | Operational performance test set-up of LED marker design..... | 14 |
| 9 | Output voltage plots for operational performance test..... | 16 |

List of tables

| | | |
|---|--|----|
| 1 | Comparison of detection ranges for conventional wire marker designs..... | 3 |
| 2 | Comparison of detection distances (in feet) for previously tested and alternative LED designs..... | 13 |

Acknowledgments

The authors would like to extend their appreciation to the following individuals: CPT Timothy C. Hartnett and CPT Wayne Miller, research aviators; Mr. Robert M. Dillard, technical assistant; and SPC Jacqueline A. Miller, crew chief. Their assistance contributed to the successful completion of the design evaluation.

This page intentionally left blank.

Introduction

In-flight wire strikes are a serious threat to U.S. Army aviation in all weather conditions during daytime and nighttime operations such as terrain flight, enclosed area takeoff and landing, and confined area maneuvering. Historically, the majority of wire strikes have occurred over familiar sites and during training missions. Despite aviator training on wire avoidance techniques, U.S. Army peacetime wire strikes, with the resultant loss of aircraft, loss of life, or injuries, remain a serious problem.

The aviation training community at Fort Rucker, Alabama, currently employs a passive marking system for increasing the conspicuity of high tension cables, electrical power lines, and telephone wires. This system uses international-orange fiberglass spheres having a diameter of approximately 11.5 inches. These spheres are attached to the cables and wires in areas heavily used by aircraft (Figure 1).

In May 1990, the U.S. Army Aeromedical Research Laboratory evaluated the current wire marker design (Figure 2a), a modification of the current design, and alternate designs for day/night conspicuity. Figure 2b shows the modified basic design which was the current sphere with 1.5 inch wide, white, high-reflectivity tape applied in a cross pattern. The alternative designs, shown in Figures 2c and 2d, had a polyhedronal shaped shell, international orange in color. One alternative marker had no additional markings (Figure 2c); one was marked with 2.5 inch diameter, circular pieces of white 3M Scotchlite™ retro-reflective tape applied to the individual faces of the polyhedron (Figure 2d); and the other was marked similarly, but with yellow-colored retroreflective tape.

Day conspicuity was performed with the naked eye, while night conspicuity included the use of image intensification (I²) devices as well as the naked eye. Results of this previous study (Levine, Rash, and Martin, 1991) demonstrated both viewing- and lighting-specific effects for each of the marker designs tested. While no differences in detection range among designs were observed under daylight conditions, improved performance under several viewing/lighting conditions was observed for the retroreflective polyhedron designs under typical aircraft lighting conditions at night. Increased detection ranges were noted both with and without I² devices and under aircraft lighting conditions characteristic of the local aviation training environment.

*See Appendix A.

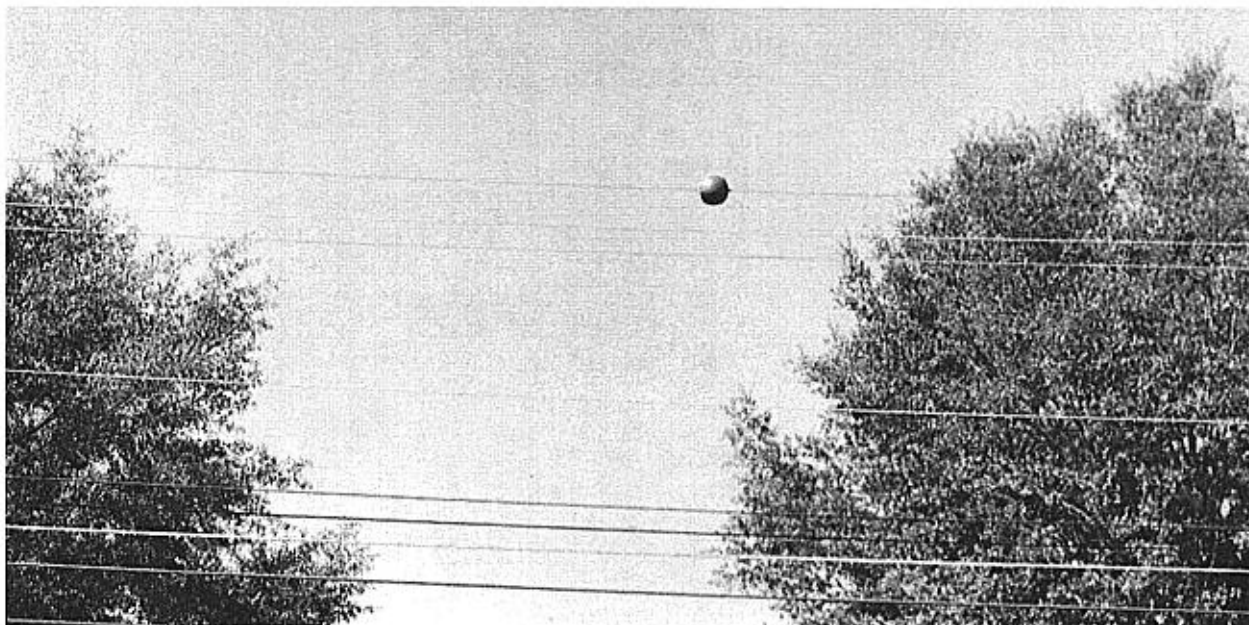


Figure 1. Current basic wire marker (international-orange sphere) mounted on power line.

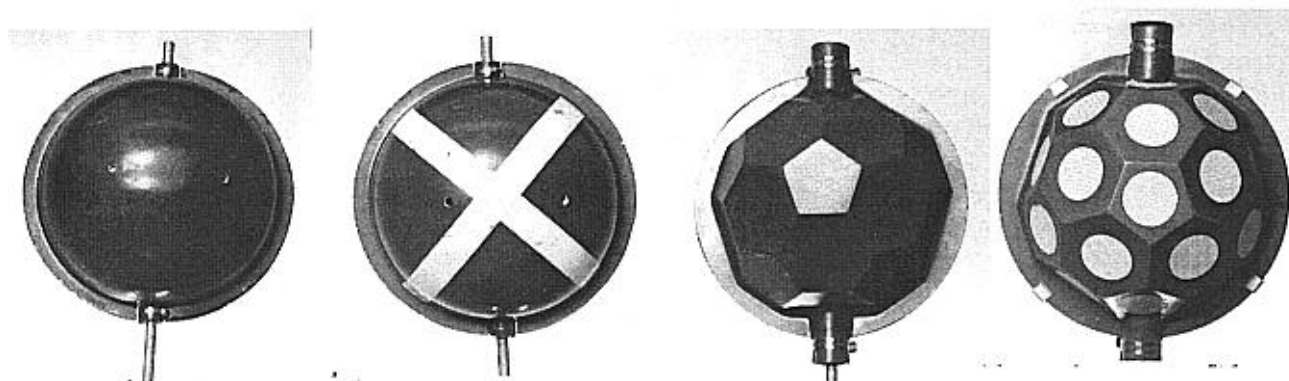


Figure 2. Wire marker test designs: (a) current uniform sphere, (b) modified sphere with reflective tape in a cross (X) pattern, (c) uniform polyhedron, (d) polyhedron with circular retroreflective tape.

Table 1.

Mean detection distances (in feet)
for conventional wire marker designs
(Levine, Rash, and Martin, 1991)

| | Basic design | Modified basic design | Reflective polyhedron design |
|---------------------------------|-----------------|-----------------------------|------------------------------------|
| <u>Day, unaided</u> | 4200* | 4200* | 4200* |
| <u>Night, unaided</u> | | | |
| Position lights | 125 | 488 | 750 |
| Anticollision lights | 213 | 688 | 1225 |
| Searchlight | 1200 | 4200* | 4200* |
| Blackout | 63 | 125 | 138 |
| <u>Night, I² 2nd</u> | | | |
| Position lights | 450 | 1250 | 1975 |
| Infrared searchlight | 525 | 1375 | 1975 |
| Blackout | 750 | 825 | 850 |
| <u>Night, I² 3rd</u> | | | |
| Position lights | 475 | 1425 | 2050 |
| Infrared searchlight | 575 | 1600 | 2250 |
| Blackout | 750 | 825 | 950 |

* Note: Maximum available range was 4200 feet.

Data in Table 1 summarize the results of the 1991 study. Mean detection distances are presented for day/night and unaided/aided viewing conditions. (Note: It should be emphasized that, because of the benign and relatively static conditions under which the data were collected, it may be erroneous to use the ranges in the data table as typical detection distances under training or operational conditions.)

A range ceiling, which existed due to restricted test space (4200 feet maximum working distance), prevented discrimination between designs for the daytime conditions. Thus, there were no observed differences in daytime detection distances among any of the tested markers within the test space. However, at a range of 4200 feet, the 11.5 inch overall diameter of the various marker designs subtended an angle of about 23.0 arc seconds. The 1.5- and 2.5-inch pieces of retroreflective tape used for visibility enhancement subtended angles of 3.0 and 5.0 arc seconds, respectively. It was suggested that detection at this range was primarily a function of color (international orange) and contrast (lighter object against a darker tree line), rather than specular reflection or detail on the surface of the shell. Therefore, differences in detectability among the marker designs would not be observed at distances greater than 4200 feet. However, heightened conspicuity could result from differences in specular reflectivity of a mobile target or when viewing from a mobile platform.

Three viewing systems were used for night testing, i.e., the unaided eye, the AN/PVS-5 night vision goggle (2nd generation I²), and the Aviator's Night Vision Imaging System-ANVIS (3rd generation I²). Each of these systems has a different spectral sensitivity. With all of these systems, the detection range of the various designs depends on the level of light, the spectral distribution of the ambient lighting, and the spectral reflective properties of the markers.

For unaided viewing in the presence of artificial lighting in the form of aircraft position and anticollision lights, the modified and alternative designs using reflective material provided the greatest detection ranges with the retroreflective polyhedron design providing nearly twice the range of the modified basic design. Under the increased directional output provided by the searchlight, the range ceiling prevented discrimination among the reflective designs -- all were equally detectable out to the maximum test range of 4200 feet. Under blackout conditions, with moonlight as the principal source of illumination, detectability among designs was considerably reduced and nearly equivalent.

Similar trends in the data were observed with I² devices, either 2nd (AN/PVS-5) or 3rd generation (ANVIS) image intensification systems. With the aircraft's position lights on steady dim or illuminated with the infrared searchlight, detection ranges with the retroreflective polyhedrons generally were superior to the basic design. Under normal low-light ambient conditions ("blackout"), no significant advantage in detectability was observed among any of the tested designs.

It is erroneous to use the ranges in the data table as absolute detection distances. However, it may be generalized that the detection range values associated with the test designs would be considered inadequate for all unaided flight conditions except for the use of the aircraft searchlight (and then only within its footprint). In addition, these designs provide only minimal increases in detection ranges for aided nighttime flight using image intensifiers.

In summary, the detection range data in Table 1 show improved detectability performance for the retroreflective polyhedron design over the current basic design for all viewing conditions. However, performance for this design was maximum (although range limited) only for unaided daytime and unaided nighttime searchlight conditions. In an attempt to achieve maximum performance for all nighttime conditions, a new wire marker design was sought. The resulting design (patent pending) features light emitting diodes (LEDs) in conjunction with retroreflective markers. This alternative design is intended to provide maximum performance for all daytime and nighttime conditions.

Technical description

System description and operation

The alternative wire marker design is intended to facilitate naked eye and electro-optical image intensification detection in daytime and nighttime/inclement weather through the use of an enhanced visual detection scheme. Enhanced detectability is achieved through the use of surface mounted retroreflective tape marking and LEDs (red or infrared). The wire marker shell is constructed of a weather resistant material, polyhedral shaped, and international orange in color. The shell serves as the housing for the internal power supply, electronic circuit board, and LED wiring harness. Figures 3 and 4 show exterior and interior views of the wire marker.

The operation of the solar powered LED wire marker is depicted in a functional block diagram in Figure 5. The functional blocks include a power supply (with power collecting, power storage, and power distribution sections), a light level detector, a power supply voltage monitor, a logic control circuit, and a visibility enhancement module.

The wire marker operates in two modes, daytime mode and nighttime/inclement weather mode, with the light level detector serving as the mode selector. When the ambient light level reaches a minimum threshold for daytime operation, the light level detector sends the appropriate signal to the logic control circuit to shut down the LED flasher circuit in the visual

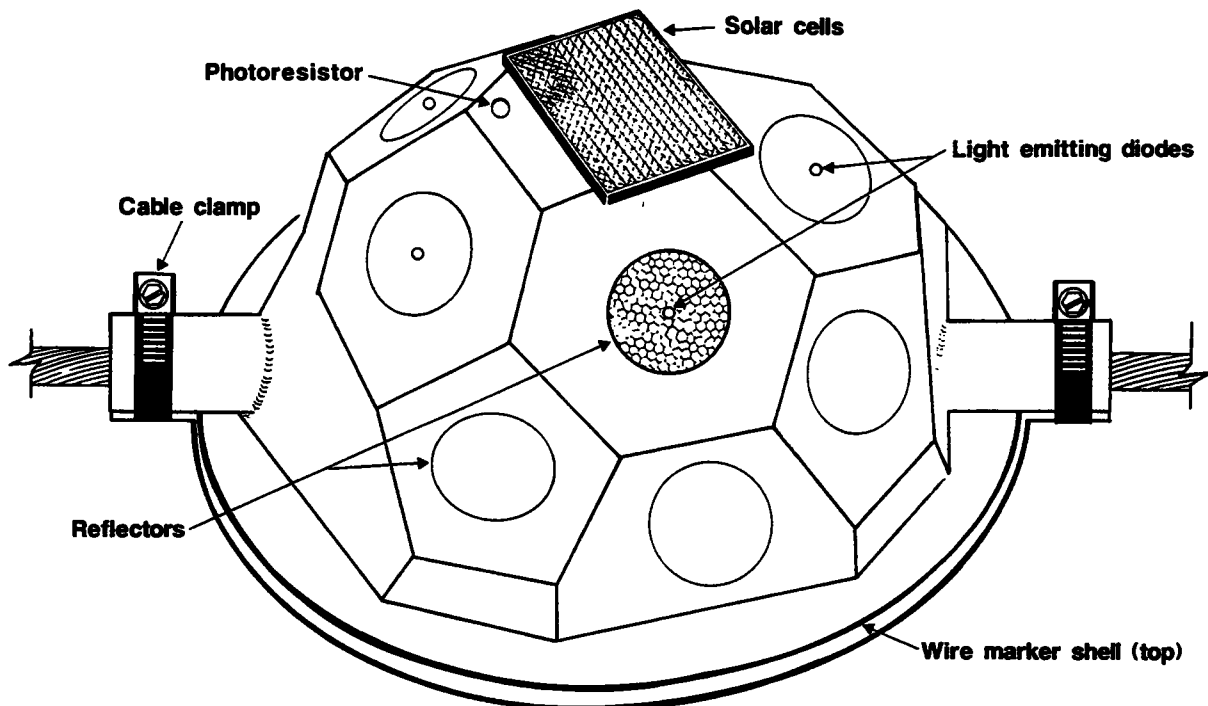


Figure 3. Exterior view of solar-powered light emitting diode wire marker design.

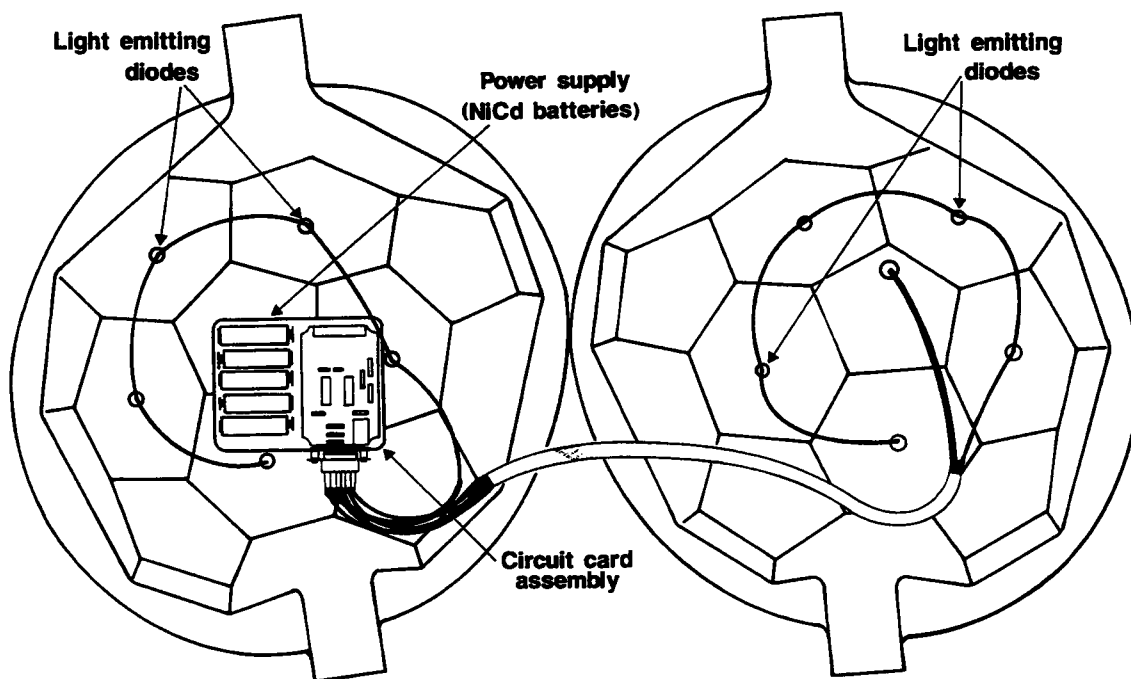


Figure 4. Interior view of solar-powered light emitting diode wire marker design.

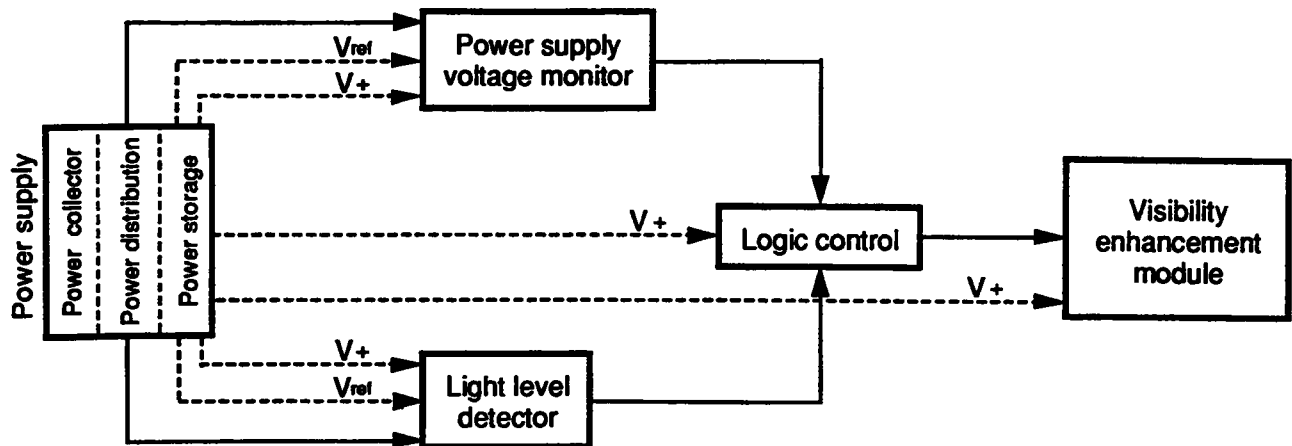


Figure 5. Wire marker design functional block diagram.

enhancement module. Alternatively, when the ambient light level drops below the threshold value, the light level detector sends appropriate logic levels to the control circuit to turn on the LED flasher circuit. Detectability of the flashing LEDs is enhanced by the retroreflective tape markers centered under each LED (see Figure 3).

The LED flasher circuit requires an operating potential of 4.0 VDC to maintain normal operation. This voltage is provided by rechargeable nickel cadmium (NiCd) batteries which are charged by the solar cells. A characteristic of NiCd batteries is consistent voltage output over the effective life of the battery. However, when power is depleted below a certain level, voltage output rapidly decreases to zero. To prevent depletion of the batteries below the circuit operating potential, the battery output voltage is continually monitored. When the battery voltage drops below 4.0 VDC, the voltage to the flashing LEDs is removed to prevent further power depletion. Excessive depletion of the NiCd batteries, which could occur during periods of continuous overcast conditions, would affect future recharging potential of the batteries.

Circuit description and operation

The solar powered LED wire marker has five distinct circuits: power supply, light level detector, power supply voltage monitor, logic control, and LED flasher. A schematic of the circuit is presented in Figure 6. A list of circuit components is provided in Appendix B.

The power supply circuit (see Figure 6) performs three functions: power collection, power storage, and power distribution. Power collection is achieved by two solar cells (3 VDC, 100 mA each) connected in series to provide 6 VDC at 100 mA. These cells are connected in parallel with four 1.2 VDC rechargeable NiCd batteries which form the power storage system.

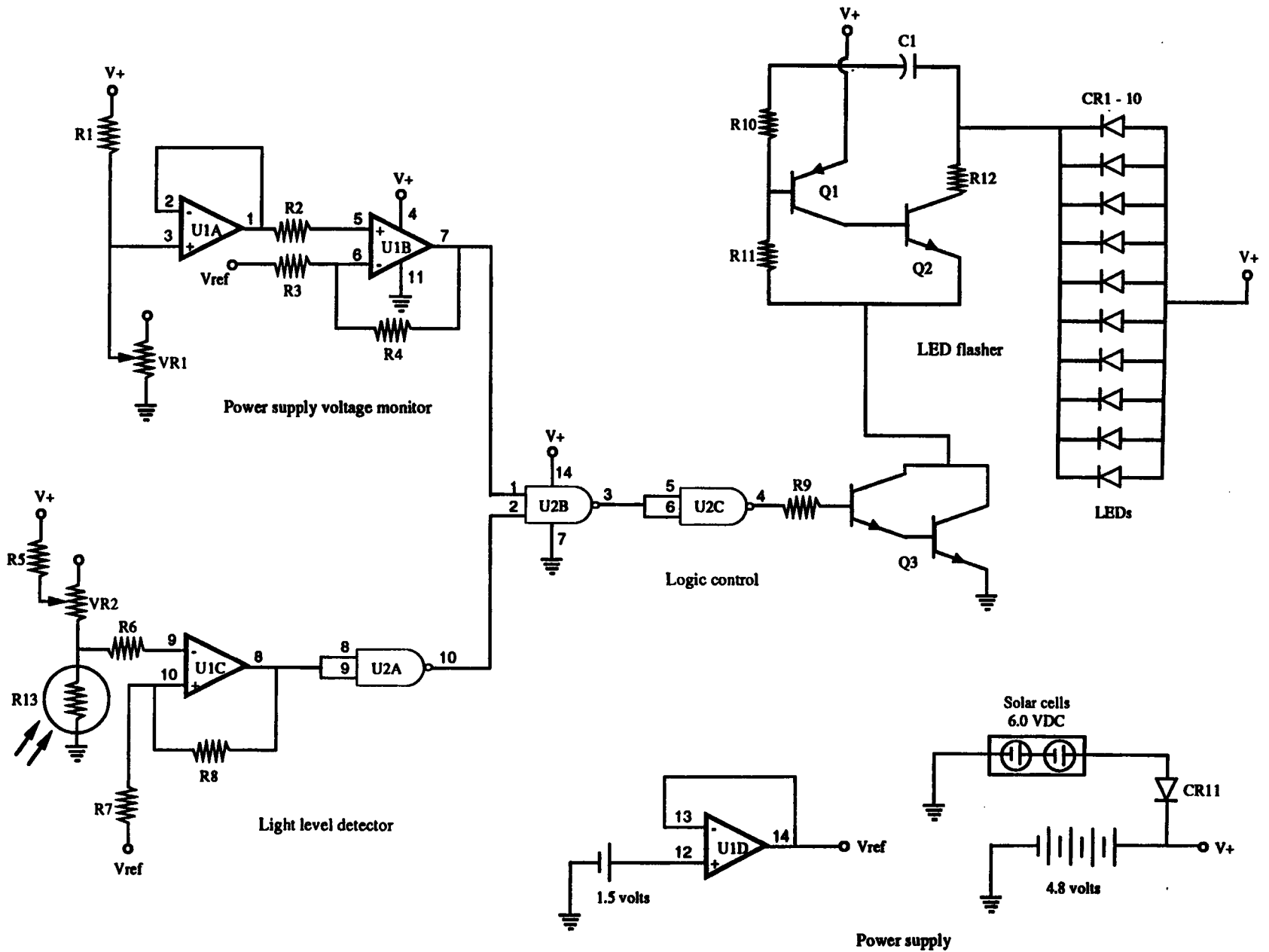


Figure 6. Schematic of solar-powered light emitting diode wire marker design.

Diode CR11 prevents battery discharge back through the solar cells during nighttime operation. The power supply provides two functional voltages. The first, V_+ , provides the positive operating voltage for all circuit components and signal voltages for the power supply voltage monitor and light level detector circuits. The second, V_{ref} , is a reference voltage used as a signal input to comparators in the power supply voltage monitor and light level detector circuits. V_{ref} is supplied by a single separate 1.5 VDC alkaline battery isolated by U1D ($\frac{1}{4}$ -LM324N), configured as a voltage follower.

The light level detector (LLD) circuit (see Figure 6) consists of a voltage divider network containing a cadmium sulfide (CdS) photoconductive cell (photoresistor), an operational amplifier (op amp) configured as a comparator, and a NAND gate used as a logic inverter. The voltage divider network, consisting of resistor R5, potentiometer VR2, and the photoresistor R13, is used to establish a voltage level at pin 9 of op amp U1C ($\frac{1}{4}$ -LM324N) which determines the point at which the transition from daytime to nighttime mode is made. For daytime operation, light falling on the photoresistor results in a low resistance value. This causes the voltage to pin 9 of U1C to go low. This low voltage at the inverting input to U1C is less than the voltage at pin 10 of U1C, the noninverting input. This latter voltage is provided from V_{ref} generated in the power supply. For these values, the output at pin 8 of U1C goes to its positive limit, V_+ . This high value is inverted by NAND gate U2A ($\frac{1}{4}$ -CD4011BE) and becomes a low logic level which is provided to the logic control circuit. For nighttime operation, the photoresistor takes on a high resistance value. This causes the voltage to pin 9 of U1C to go high. This high voltage at the inverting input to U1C is greater than the voltage at pin 10 of U1C. For these values, the output at pin 8 of U1C goes to its negative limit. This low value is inverted by NAND gate U2A and becomes a high logic level which is provided to the logic control circuit. Potentiometer VR2 is used to adjust the daytime/nighttime transition point.

The power supply voltage monitor (PSVM) circuit (see Figure 6) consists of a voltage divider network and two op amps configured as comparators. The voltage divider consists of resistor R1 and potentiometer VR1 connected to V_+ (4.8 VDC). The setting of VR1 determines the minimum battery voltage value (4.0 VDC) below which the flashing LEDs are disabled. This voltage is isolated by U1A ($\frac{1}{4}$ -LM324N), configured as a voltage follower, and applied to pin 5 of U1B ($\frac{1}{4}$ -LM324N). The voltage at pin 5 is compared to V_{ref} applied at pin 6 of U1B. When the battery voltage exceeds 4.0 VDC, the output at pin 7 of U1B goes high (greater than 3 VDC) and this level is provided to the logic control circuit. When the battery voltage drops below 4.0 VDC, the output of U1B goes low (less than 0.5 VDC).

The logic control circuit (see Figure 6) consists of two NAND gates. Logic level outputs from the PSVM and LLD circuits are applied to pins 1 and 2 of NAND gate U2B ($\frac{1}{2}$ -CD4011BE), respectively. The output of U2B (pin 3) is applied to pins 5 and 6 of U2C ($\frac{1}{2}$ -CD4011BE) which is configured as an inverter. NAND gates U2B and U2C operate together to provide an AND function of the two inputs to the logic control circuit. As long as the power supply NiCd battery voltage level is greater than 4.0 VDC, the output of the logic control circuit (pin 4 of U2C) is determined by the LLD circuit output (low for daytime and high for nighttime). If the NiCd battery voltage drops below 4.0 VDC, the resulting low input at pin 1 of U2B causes the output at pin 4 of U2C to go low. Due to the AND gate operation of the logic control circuit, its output at pin 4 of U2C is high only for the conditions of nighttime illumination and a battery voltage of greater than 4.0 VDC.

The LED flasher circuit (see Figure 6) consists of 10 LEDs, an emitter follower, a resistance-capacitance (RC) timing circuit, and several biasing and current limiting resistors. The LEDs (CR1-10) are connected together in a parallel array. The LED array is in series with V+, the timing circuit, and the emitter follower (Q3), which operates as the on/off switch for the entire LED flasher circuit. The output of the logic control circuit, applied through R9, controls the bias on Q3. For nighttime conditions and when sufficient battery voltage is available, the resulting high level at the base of Q3 forward biases Q3 and causes it to conduct. This applies a ground potential to the emitter of Q2 and the base of Q1 through resistor R11. This activates the flasher timing circuit. Transistor Q1 then is biased on and off as determined by the RC time constant of resistor R10 and capacitor C1. The on and off biasing of Q1 controls the conduction of transistor Q2 which, during a portion of the period of the RC timing cycle, applies the ground potential to the LEDs through resistor R12. The LEDs are on during this period.

Bench test

Prior to full scale testing, the operational lifetime of the wire marker power supply circuit was evaluated under sustained no-light conditions. This is of interest because extended periods of inclement weather may leave the circuit switched in the nighttime (flashing) mode and not allow the solar cells to adequately recharge the NiCd cells.

The bench test was performed on a breadboard circuit with the solar cells mounted to the side. Testing was performed in a closed, unlit room. A Grant Squirrel 1200 series meter/logger was used to monitor voltages at four points in the circuit. Four channels were used to monitor the NiCd battery voltage (V+), V_{ref}

voltage (pin 14 of U1D), the power supply voltage monitor voltage (pin 7 of U1B), and the light level detector voltage (pin 10 of U2A). See Figure 6 for pin locations.

Voltage data were collected continuously over a 4-day (99 hours) period with sample readings collected and recorded at 1-minute intervals. The initial values of each parameter were V+ power supply voltage 5.29 VDC, V_{ref} voltage 1.15 VDC, PSVM voltage 3.96 VDC, and LLD voltage 4.93 VDC. Plots of these voltage data are presented in Figure 7.

Since all of the test voltages with the exception of V_{ref} were derived from V+, it was expected that changes in the power supply voltage monitor and light level detector would track with changes in V+. The curves in Figure 7 support this expectation. V+ showed a very gradual and linear decline over the first 75 hours. The rate of decline from 5.29 to 4.77 VDC during this period was approximately 7 millivolts per hour. Over the next 35 minutes, V+ dropped to 4.05 VDC at a rate of 1.4 volts per hour. Additional rapid decline occurred at 78 hours (declining to 2.98 VDC) and 85 hours (declining to 2.6 VDC). The photoresistor and PSVM output voltages showed similar trends in decline. V_{ref} , supplied by a separate battery, was unaffected by the declining V+. The test was concluded at 99 hours with final readings of 2.4 VDC at V+ and 1.15 VDC at V_{ref} .

Field test

Detection performance

During the conspicuity study cited previously, the LED design was added as an additional test design. In this test design, red LEDs were used and tested under all day/night and unaided/aided test conditions. For enhanced I^2 detectability, infrared LEDs can be used. Table 2 repeats the mean detection distances of the previously described basic and alternative designs (from Table 1). An additional column presents the detection range data of the LED design for comparison.

Each mean detection distance for the LED design was 4200 feet (the ceiling value for the test range), equaling or exceeding the values for the other test designs for every test condition. In a followup evaluation of the LED design for maximum detection ranges during operational flight, USAARL aviators reported being able to observe the marker with the naked eye at a distance of approximately 1000 feet at an altitude of 200 feet above ground level (AGL), approaching at 70 knots (kts).

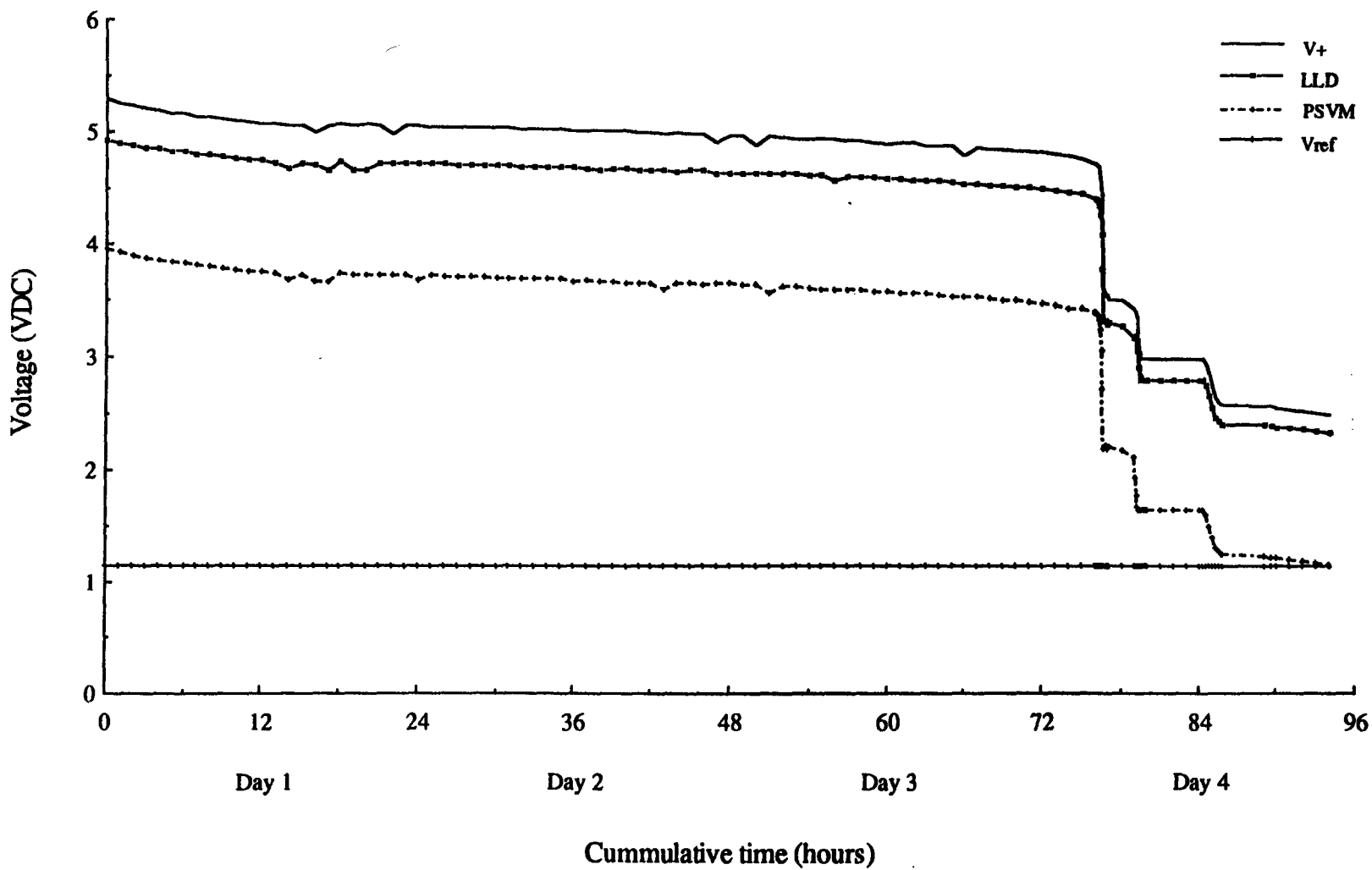


Figure 7. Output voltage plots for bench test.

Table 2.

**Comparison of detection distances (in feet)
for previously tested and alternative LED designs**

| | Basic design | Modified basic design | Reflective polyhedron design | LED design |
|---------------------------------|-----------------|-----------------------------|------------------------------------|---------------|
| <u>Day, unaided</u> | 4200* | 4200* | 4200* | 4200* |
| <u>Night, unaided</u> | | | | |
| Position lights | 125 | 488 | 750 | 4200* |
| Anticollision lights | 213 | 688 | 1225 | 4200* |
| Searchlight | 1200 | 4200* | 4200* | 4200* |
| Blackout | 63 | 125 | 138 | 4200* |
| <u>Night, I² 2nd</u> | | | | |
| Position lights | 450 | 1250 | 1975 | 4200* |
| Infrared searchlight | 525 | 1375 | 1975 | 4200* |
| Blackout | 750 | 825 | 850 | 4200* |
| <u>Night, I² 3rd</u> | | | | |
| Position lights | 475 | 1425 | 2050 | 4200* |
| Infrared searchlight | 575 | 1600 | 2250 | 4200* |
| Blackout | 750 | 825 | 950 | 4200* |

* Note: Maximum available range was 4200 feet.

With 3rd generation image intensifiers (ANVIS), with and without anticollision lights on, the marker was observed at a distance of approximately 4300 feet at an altitude of 250 feet AGL, approaching at 70 kts. In this evaluation, the wire marker was positioned at a height of 25 feet AGL and oriented as it would be on a wire or cable. Local weather conditions were temperature of 77° F, dew point of 71° F, and relative humidity of 83 percent with scattered cloud cover at 4000 feet.

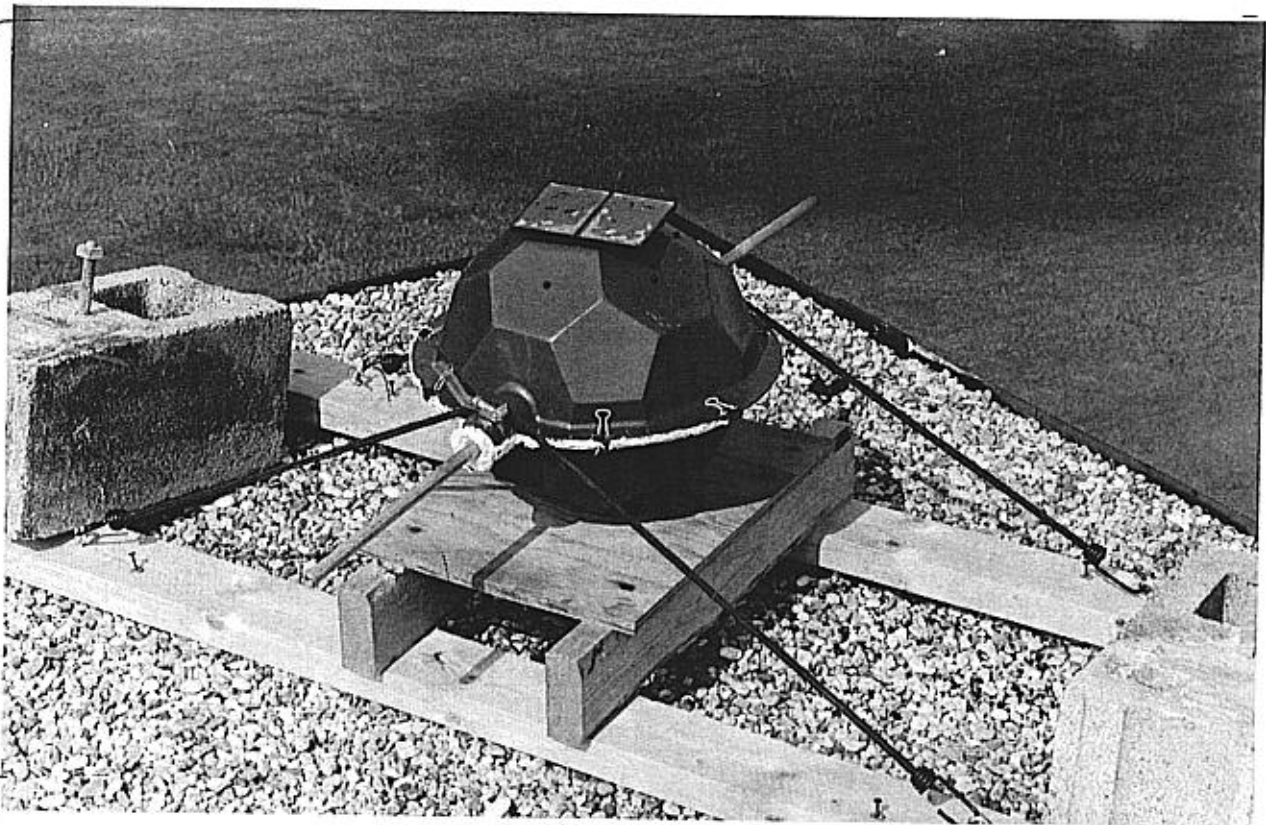


Figure 8. Operational performance test set-up of LED marker design.

Operational performance

To test the functionality of the integrated circuit for mode selection and continuous operation, a fully integrated wire marker circuit was tested in the polyhedronal shell under operational conditions. Figure 8 shows the marker setup for the operational performance testing.

Operational testing was staged at the U.S. Army Aeromedical Research Laboratory (latitude 31°10'N, longitude 85°26'W, altitude 25' AGL). The test area was a location on the roof of the building, unobscured from the sun. During the simulated operational testing, the integrated marker was maintained continually in the test area. The test was started on 10 July 1992 and ended on 14 July 1992. During this period, meteorological sunrise occurred at 0548 and sunset occurred at 1949.

A Grant Squirrel 1200 series meter/logger was used to monitor and record voltages at four points in the circuit. Four channels were monitored for solar cell voltage, NiCd battery voltage (V+), PSVM voltage (pin 7 of U1B), and LLD voltage (pin 10 of U2A).

Voltage data were collected continuously over a period of 96 hours beginning at 1424 on 10 July. Sample readings were taken every minute, and at each $\frac{1}{2}$ -hour interval, the readings were averaged and recorded by the meter/logger. The initial values of each parameter were solar cell voltage 5.84 VDC, NiCd battery (V+) voltage 5.32 VDC, PSVM voltage 4.02 VDC, and LLD op amp voltage 0.00 VDC. Plots of the voltage data recorded over the test period are presented in Figure 9.

Figure 9 shows that the weather over the test period was generally sunny to partly cloudy and 1 day was overcast with rain. Although not ideal, this weather is typical of operational conditions. During the daytime, the solar cells did not reach full potential (6.0 VDC), but they maintained average values of 5.49 VDC to 5.75 VDC which was adequate to charge the four 1.3 volt batteries. As ambient lighting was reduced or increased, the solar cell voltages gradually changed towards a low value of zero volts or a high value of six volts, respectively. Data showed that the most significant rates of voltage change occurred in the two 30-minute periods prior to switch to nighttime mode, and in the one 30-minute period subsequent to switch to daytime mode. During the day, small voltage fluctuations occurred due to cloud cover.

While the solar cell voltages were above the total NiCd battery voltage (5.2 VDC), the batteries (V+) were charged. This was indicated by the rise in V+ during the daytime and the gradual decline as the sun set into the nighttime. The average daytime voltages of V+ ranged from 5.35 VDC to 5.40 VDC, and the average nighttime voltages ranged from 5.12 VDC to 5.16 VDC. Throughout this testing period, the batteries maintained a voltage no lower than 5.03 VDC, which occurred at the end of a nighttime cycle.

Because the power supply voltage monitor circuit was designed to monitor the battery voltage, the increases and decreases in V+ voltage were reflected in the PSVM. The PSVM average daytime voltage values ranged from 4.08 VDC to 4.12 VDC, and the average nighttime voltage values ranged from 3.81 VDC to 3.83 VDC. The PSVM and V+ voltages consistently differed by approximately 1.31 volts and, since the V+ voltage remained above 4.00 VDC throughout the test period, the PSVM voltages never dropped below 3.00 volts (as designed).

In the daytime, the photoresistor in the light level detector circuit had a low resistance value so that the LLD voltage had a value of zero. At nighttime, the average voltages ranged from 5.09 VDC to 5.12 VDC. The voltages across the LLD circuit at night were equivalent to the V+ voltages until transition occurred.

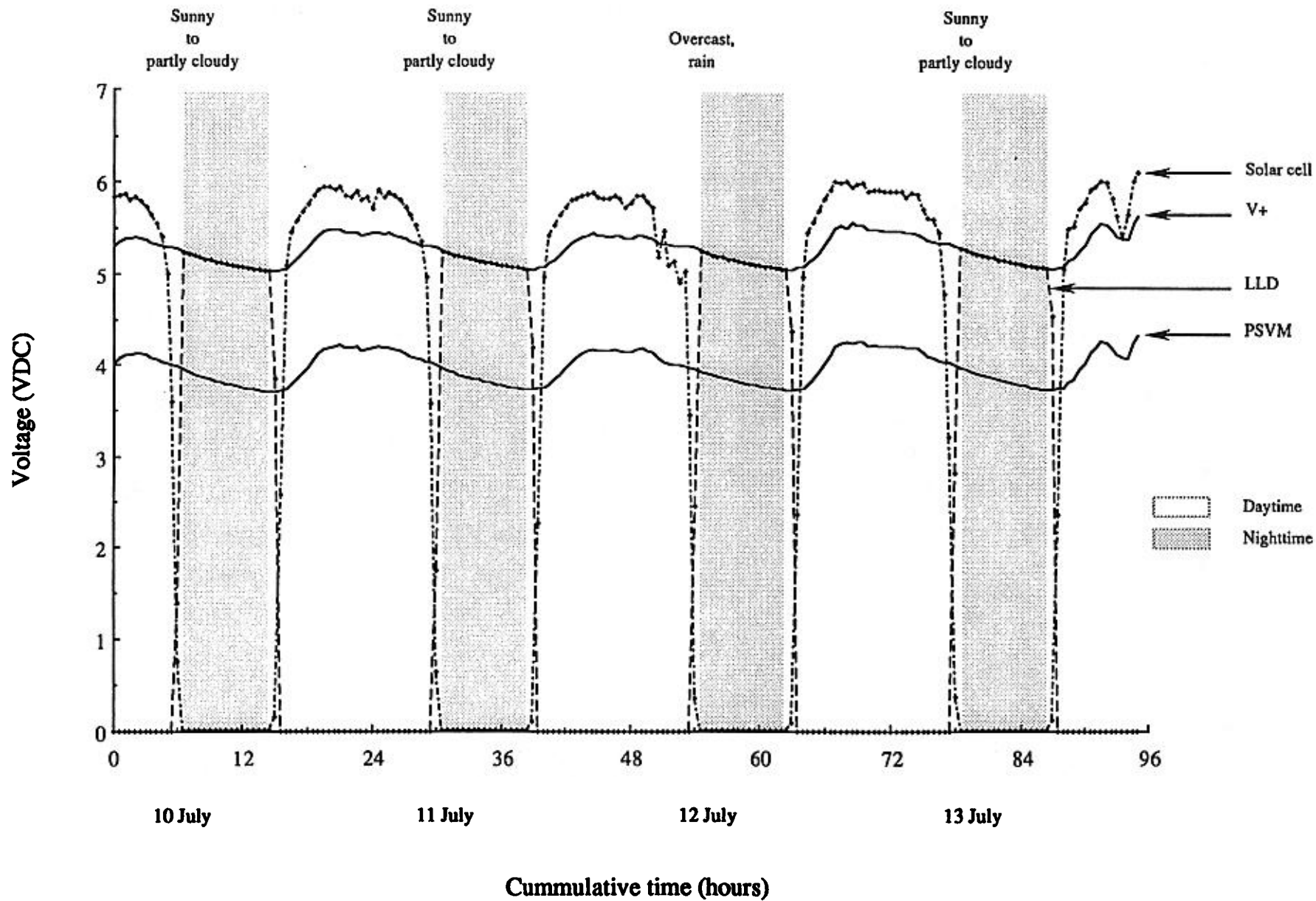


Figure 9. Output voltage plots for operational performance test.

The transition from daytime to nighttime mode was instantaneous once the ambient lighting fell below a level determined by the user. Under normal operation, the light level detector circuit controlled the switch. In the daytime, the photoresistor in the LLD circuit had a low resistance value of zero. At nighttime, the average voltages ranged from 5.09 to 5.12 VDC. The nighttime voltages were equivalent to the V+ voltages until transition occurred. The curve of LLD in Figure 9 has a sloped appearance due to the averaging of voltages over a 30-minute period. The transition between modes occurred in the last 30 minutes of each day/night period. From the data, a switch was determined to have occurred when voltage values of the LLD circuit rose to the V+ voltage (transition to night mode) or dropped below the V+ voltage (transition to day mode).

During the test period, the temperature and humidity were high. The photo in Figure 8 shows some condensation occurring inside the solar cell packages. Data showed that the performance of the solar cells was not affected by the moisture. On the afternoon of the third testing day, an episode of torrential rain occurred where the solar cell voltages changed irregularly (see Figure 9) due to heavy intermittent overcast. Data on the following day appeared nominal and water was not found inside the marker shell at the conclusion of testing.

Summary

The self-powered light emitting diode wire marker is an alternative marker intended for use in indicating the presence of cables and/or wires located at heights above the ground which could be potential aviation hazards. Current wire markers employ an international-orange color with reflective or retroreflective marking patterns to augment visibility and detection range. This alternative marker design enhances visibility and detection range over the current design through the use of active emission light emitting diodes which are visible to the naked eye and image intensification systems.

Enhanced detectability is the predominant advantage of this alternative wire marker design. Another significant feature of this LED marker is the powering circuit which is designed to recharge itself and automatically select the operating mode based on ambient lighting conditions. A photodetector monitors ambient light levels and regulates switching between daytime mode (when the solar cells recharge the batteries and the LEDs are switched off) and nighttime/adverse weather mode (when the LEDs are switched on to flash).

In a controlled laboratory bench test of the powering circuit, it was determined that four rechargeable NiCd batteries were capable of supporting the circuit in continuous nighttime

(LED flashing) mode for a period of 75 hours before unrecoverable failure of the batteries occurred. Operational performance testing showed that two 3-volt solar cells were sufficient for maintaining battery charge under normal operating conditions, and that the mode selection circuit operated successfully in switching the circuit for most efficient operation over five periods of daytime and four periods of nighttime operation. This test also showed that the shell integrated with the solar cells, photo-detector, and LEDs provided protection from heat and water.

Results of the bench test and operational performance test indicate that this alternative self-powering LED wire marker system is a feasible alternative for current markers to provide low-maintenance, enhanced detectability of wire and/or cable hazards to aviation.

Reference

Levine, R. R., Rash, C. E., and Martin, J. S. 1991.
Conspicuity comparison of current and proposed U.S. Army
wire marker designs. USAARL Report No. 91-9.

Appendix A.

List of manufacturers

3M Traffic Control Materials Division
Building 223-3N-01, 3M Center
St. Paul, MN 55144-1000

Grant Instruments (Cambridge) Ltd.
Barrington, Cambridge CB2 5QZ England
for Science/Electronics
2277 Maue Rd.
Miamisburg, Ohio 45342

Appendix B.

List of components

C1 Capacitor, electrolytic, 4.7 μ F, 35 V
CR1-10 Light emitting diode, CX556R
CR11 Diode, germanium, 1N34A, 75 V PIV
Q1 Transistor, 2N2907
Q2 Transistor, 2N2222
Q3 Transistor, ECG265, Darlington
R1 Resistor, 100K Ω , $\frac{1}{4}$ watt, 1%
R2, R6 Resistor, 39K Ω , $\frac{1}{4}$ watt, 1%
R3, R7 Resistor, 47K Ω , $\frac{1}{4}$ watt, 1%
R4, R8-11 Resistor, 1K Ω , $\frac{1}{4}$ watt, 1%
R5 Resistor, 33K Ω , $\frac{1}{4}$ watt, 1%
R12 Resistor, 10 Ω , $\frac{1}{4}$ watt, 5%
U1A Quad op amp, LM324N
U2A Quad NAND gate, CD4011BE
VR1-2 Potentiometer, 100K Ω , 15 turn, $\frac{3}{4}$ watt

Battery alkaline, 1.5 VDC

Battery (4) NiCd, rechargeable, 1.2 VDC

CdS cell photoconductive cell (photoresistor), CL703L/2,
dual element

Photovoltaic

Cell (2) Solar cell, 3 VDC, 100 mA